Biogeosciences, 7, 777–793, 2010
www.biogeosciences.net/7/777/2010/

Biogeosciences

Atmospheric deposition of nutrients and excess N formation in the North Atlantic

L. M. Zamora[1], A. Landolfi[2], A. Oschlies[2], D. A. Hansell[1], H. Dietze[2], and F. Dentener[3]

[1]Rosenstiel School of Marine and Atmospheric Science, University of Miami, Miami, USA
[2]IFM-GEOMAR, Leibniz-Institut für Meereswissenschaften an der Universität Kiel, Kiel, Germany
[3]European Commission, Institute for Environment and Sustainability, Joint Research Centre, Ispra, Italy

Received: 16 September 2009 – Published in Biogeosciences Discuss.: 14 October 2009
Revised: 27 January 2010 – Accepted: 3 February 2010 – Published: 26 February 2010

Abstract. Anthropogenic emissions of nitrogen (N) to the atmosphere have been strongly increasing during the last century, leading to greater atmospheric N deposition to the oceans. The North Atlantic subtropical gyre (NASTG) is particularly impacted. Here, upwind sources of anthropogenic N from North American and European sources have raised atmospheric N deposition to rates comparable with N_2 fixation in the gyre. However, the biogeochemical fate of the deposited N is unclear because there is no detectable accumulation in the surface waters. Most likely, deposited N accumulates in the main thermocline instead, where there is a globally unique pool of N in excess of the canonical Redfield ratio of 16N:1 phosphorus (P). To investigate this depth zone as a sink for atmospheric N, we used a biogeochemical ocean transport model and year 2000 nutrient deposition data. We examined the maximum effects of three mechanisms that may transport excess N from the ocean surface to the main thermocline: physical transport, preferential P remineralization of sinking particles, and nutrient uptake and export by phytoplankton at higher than Redfield N:P ratios. Our results indicate that atmospheric deposition may contribute 13–19% of the annual excess N input to the main thermocline. Modeled nutrient distributions in the NASTG were comparable to observations only when non-Redfield dynamics were invoked. Preferential P remineralization could not produce realistic results on its own; if it is an important contributor to ocean biogeochemistry, it must co-occur with N_2 fixation. The results suggest that: 1) the main thermocline is an important sink for anthropogenic N deposition, 2) non-Redfield surface dynamics determine the biogeochemical fate of atmospherically deposited nutrients, and 3) atmospheric N accumulation in the main thermocline has long term impacts on surface ocean biology.

Correspondence to: L. M. Zamora
(lzamora@rsmas.miami.edu)

1 Introduction

Atmospheric deposition of N to the ocean has greatly increased over the past 200 years with the intensification of anthropogenic N production from agricultural and fossil fuel sources (Duce et al., 2008; Galloway, 2008). The North Atlantic subtropical gyre (NASTG) is particularly affected by increased deposition because it is very nutrient impoverished and it is located downwind of highly industrialized continents. As atmospheric N deposition to the NASTG has more than doubled since 1860 (Galloway, 1996), the process has become an increasingly important new source of N to marine organisms there (Krishnamurthy et al., 2007).

The fate of atmospheric N deposited in the NASTG is unclear because the nutrient dynamics are incompletely understood. Phosphate concentrations at the surface are very low (often <1 nM) (Wu et al., 2000; Li and Hansell, 2008), and because deposition has high N:P ratios, typically ranging from 100:1 to 300:1 (e.g. Markaki et al., 2003; Chen et al., 2007), one might expect deposited N to accumulate in the surface waters before being transported from the surface into the main thermocline via subduction (or sinking). Although we cannot exclude changes on longer timescales, increases in the concentrations of N have not been observed in the gyre surface in the past 20 years (Fig. 1). This lack in increase in surface N indicates that the estimated 0.1 mol N m^{-2} yr^{-1} (obtained from Dentener et al., 2006) deposited to the surface is removed at a rate approximating its input.

Published by Copernicus Publications on behalf of the European Geosciences Union.

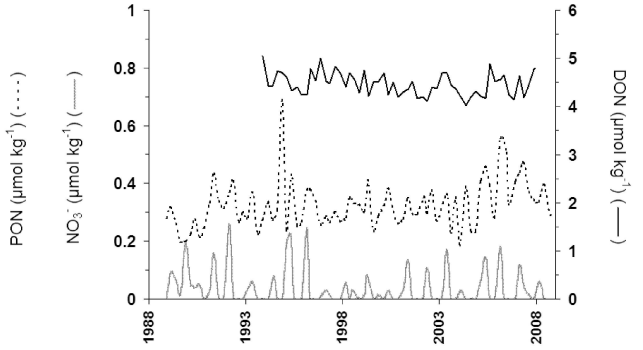

Fig. 1. Four-month seasonally averaged surface concentrations of nitrate (NO_3^-), particulate organic nitrogen (PON) and dissolved organic nitrogen (DON) at the Bermuda Atlantic Time-series Study station from 1988 through 2008. No noticeable increase in dissolved or particulate N is observed.

Export to the main thermocline is one apparent fate for excess N deposited to the subtropical North Atlantic. In the depth range of 200–800 m (Fig. 2), high inorganic N:P ratios relative to Redfield values (16N:1P on a molar basis) (Redfield et al., 1963) have long been noted (Fanning, 1992). The indices N*, DINxs and TNxs have been used to describe the N in excess of the canonical Redfield ratio (Gruber and Sarmiento, 1997; Hansell et al., 2004; Landolfi et al., 2008). TNxs, which includes organic nitrogen and phosphorus, would be the ideal index to use to describe basin-wide biogeochemistry because organic matter is an important pool of nutrients at the surface (Fig. 1; Bronk, 2002; Karl and Björkman, 2002). However, because there are not enough dissolved organic nitrogen (DON) and phosphorus (DOP) data to meaningfully map distributions in the NASTG, and because the organic DON and DOP fractions in deposition are not well understood, here we restrict ourselves to the use of inorganic N and P. We employ the index DINxs, which is defined as the excess of inorganic N relative to inorganic P expected from the Redfield relationship:

$$\mathrm{DINxs} = [\mathrm{NO_3^-}] - 16 * [\mathrm{PO_4^{3-}}] \quad (1)$$

The difference between DINxs and the definition of N* (Gruber and Sarmiento, 1997) as modified by Deutsch et al. (2001) is the constant 2.9:

$$\mathrm{N^*} = \mathrm{DINxs} + 2.9 \quad (2)$$

The constant 2.9 imposes a global mean N* value of zero, but the spatial gradients of the excess nitrate are the same, whether calculated as N* or DINxs. Because here we focus only on the North Atlantic and for this reason do not require the global mean N* value to be zero, we use DINxs instead of N*.

Along with the input of high N:P atmospheric material, other suggested sources of elevated DINxs levels in the NASTG include mineralization of high N:P diazotrophic particles and subduction of high N:P dissolved organic matter (DOM) (Fanning, 1992; Gruber and Sarmiento, 1997; Pahlow and Riebesell, 2000; Deutsch et al., 2007; Hansell et al., 2007). The relative contributions of atmospheric N deposition and N_2 fixation are particularly difficult to determine (Hansell et al., 2007) because both inputs have similar biogeochemical signatures (i.e., light isotopic N signatures (Knapp, 2010) and high N:P ratios). Another unknown is the mechanisms for excess N from N_2 fixation and atmospheric deposition to reach the depths of the main thermocline from the surface layer.

Both the biological response and the physical transport of water are key to the eventual fate of the deposited nutrients. Thus, in the present study we examine three of the most likely transport mechanisms: transport by advection and subduction, preferential P remineralization in sinking particles, and non-Redfield nutrient uptake and export in phytoplankton (Fig. 3). The first mechanism is simple physical transport of deposited excess N, assessed here in what we call the "Redfield scenario". If all biological processes occur in Redfield ratios, then deposited excess N should be retained in the surface layer until it is either transported out of the system by advection or to depth through physical processes like subduction. Any deposited N not taken up by and retained in the biological system (i.e., as biomass at Redfield ratio) would then act similarly to a passive tracer, perhaps being present as DON in the real ocean, following uptake and release by the autotrophs.

The second mechanism for transport of excess N to depth occurs when P is preferentially remineralized in the surface with respect to N (referred to here as the "preferential P remineralization scenario"). If P is more readily mineralized from sinking biogenic particles than N, a particle initially at Redfield N:P ratios will become N-enriched as it sinks. In this scenario, phosphorus would be more efficiently recycled and retained in surface waters, lessening P depletion and enabling continued production with further N deposition. At the same time, sinking N-enriched particles would keep surface water N levels low, and upon mineralization in the main thermocline would form the enriched DINxs signal found there. Evidence of differential remineralization rates comes from vertical gradients in the molar ratios of DON and DOP (Vidal et al., 1999; Abell et al., 2000; Aminot et al., 2004; Landolfi et al., 2008). N:P enrichment of particles at depth may also be partially explained by preferential P remineralization (Antia, 2005).

The third mechanism for the transport of atmospheric excess N to the main thermocline is through the growth and sinking of particles that are formed at higher than Redfield ratios (referred to here as the "excess N uptake scenario"). This process is hypothesized to be caused by changes in the optimal biochemical makeup of phytoplankton under nutrient stress (Arrigo, 2005; Pahlow and Oschlies, 2009), and has been observed in some phytoplankton in the NASTG (e.g.

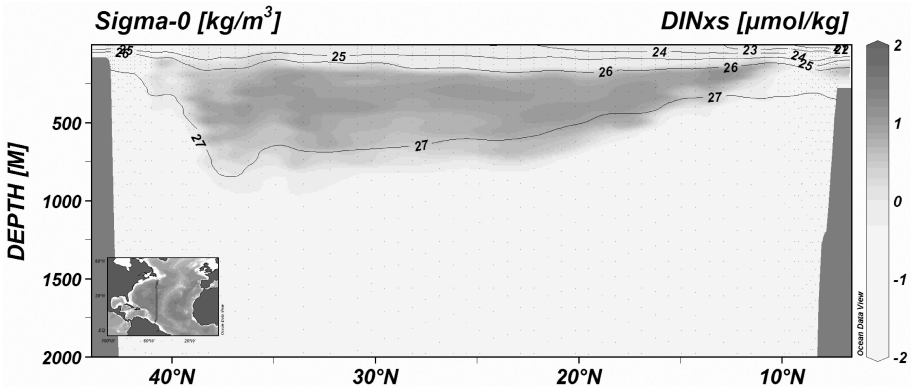

Fig. 2. Distribution of DINxs (gray scale) and sigma theta (line) from the 2003 CLIVAR A20 section. A high DINxs pool is observed between 26 and 27σ_θ (approximately 200–800 m).

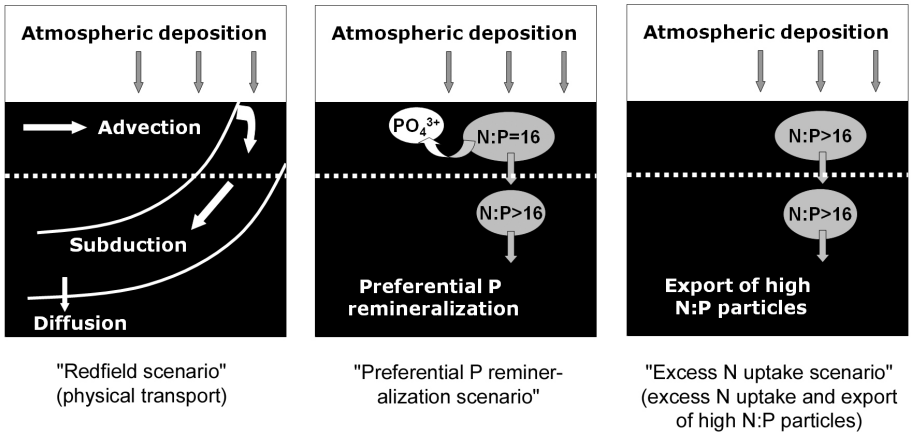

Fig. 3. Three mechanisms for the transport of atmospherically-deposited nutrients from the surface to below the ocean surface mixed layer. Nutrient deposition enhances biomass growth in all three scenarios. When biomass has Redfield N:P ratios (Redfield scenario), only vertical mixing can move from the surface to the main thermocline the high N:P material deposited from the atmosphere that remains after biological uptake. In the preferential P remineralization scenario, biomass loses phosphate preferentially as it sinks so that the remineralization of high N:P sinking particles at depth contributes to the DINxs pool. In the excess N uptake scenario, particles are produced and exported at high N:P ratios. Any of these scenarios could contribute to the transport of atmospheric nutrients from the surface to the main thermocline.

Lomas et al., 2004; Van Mooy et al., 2009). The high N:P ratios of particles found in sediment traps could also be explained, at least in part, by this process.

The three scenarios are expected to result in markedly different vertical gradients when implemented in a model, both at the surface and in the main thermocline. We used a 3-D global biogeochemical-ocean transport model to isolate the simulated effects of these three mechanisms. By observing the biogeochemical signatures of the three mechanisms in the water column, we are able to 1) identify which mechanisms best simulate the observed nutrient patterns, 2) compare the production rates of DINxs and ADINxs (where ADINxs is the fraction of the DINxs pool in the main thermocline coming from atmospheric deposition), and 3) approximate the importance of atmospheric deposition to total excess N formation in the main thermocline of the subtropical North Atlantic. Overall, we seek to better assess the functioning of the North Atlantic subtropical gyre nutrient system and how it may respond in the future to increased N inputs from the atmosphere.

2 Methods

2.1 Atmospheric nutrient deposition to the ocean

Year 2000-level deposition of wet and dry inorganic nitrogen was obtained at a one degree resolution from the mean of 23 atmospheric chemistry transport models (Dentener et al., 2006). Compared to measurements, the mean model showed relatively good performance over the North American and European source regions; also comparison over the few available coastal and open ocean measurements was relatively

good (Dentener et al., 2006). Inorganic nitrogen deposition (Fig. 4a) applied to the biogeochemical ocean model included NO_y (NO, NO_2, HNO_3, HNO_4, NO_3, $2{\cdot}N_2O_5$, PAN, organic nitrates) and NH_x (NH_3 and NH_4).

Observations of soluble reactive phosphorus (SRP) deposition are sparse; therefore, instead of modeling SRP directly, it was assumed that all/total phosphorus deposition was in the form of bioavailable SRP. Our motivation for making this assumption was twofold: first, there are more total phosphorus (TP) data available than there are SRP data, and so the accuracy of the modeled P deposition was easier to gauge by using TP data as a basis for comparison. Secondly, because in reality, SRP is much lower than TP (between 7–100%, averaging ∼32% in the North Atlantic, Mahowald et al., 2008; Baker et al., 2006a,b), we intended this method to err by overestimating the amount of bioavailable P deposition to the ocean. Thus, any errors due to faulty P deposition would be more likely to underemphasize the role of excess N deposition rather than falsely over-emphasize it, leading to a conservative estimate of how deposition affects the relevant biogeochemical processes studied in this experiment.

Since the two main sources of total phosphorus in deposition are dust and combustion processes (Mahowald et al., 2008), we estimated TP deposition (Fig. 4b) from maps of dust and black carbon (BC) (BC is a proxy for combustion sources). We assume that TP in aerosol particles is equally divided between coarse and fine size fractions. The two size fractions have different compositions; taking this into account, we use published BC:TP molar ratios of 0.02 for coarse particles and 0.0029 for fine particles (Mahowald et al., 2005) in order to obtain the final value of TP in the deposition. P derived from dust was estimated from a dust:TP ratio of 7×10^{-4} (Taylor and McLennan, 1995). BC and dust deposition maps were averaged from five atmospheric chemistry models made available by the AeroCom project (the GISS, LOA, LSCE, MATCH, and PNNL models).

The contribution of organic N in deposition was not included in the model. Soluble organic nitrogen in deposition is likely to be at least partially bioavailable (Peierls and Paerl, 1997; Seitzinger and Sanders, 1999; Duarte et al., 2006) and has been estimated to be ∼30% of the inorganic N values (Duce et al., 2008), although sources to the subtropical North Atlantic may be less than that (Zamora et al., 2009). The sources, distributions, bioavailability and lifetime of these compounds, however, are not well known. Therefore, organic N compounds other than organic nitrates were excluded. Even less is known about soluble organic P in deposition, but the existing literature indicates that organic P does not outweigh the large excess of N with respect to Redfield ratios (e.g. Graham et al., 1979; Chen et al., 2007).

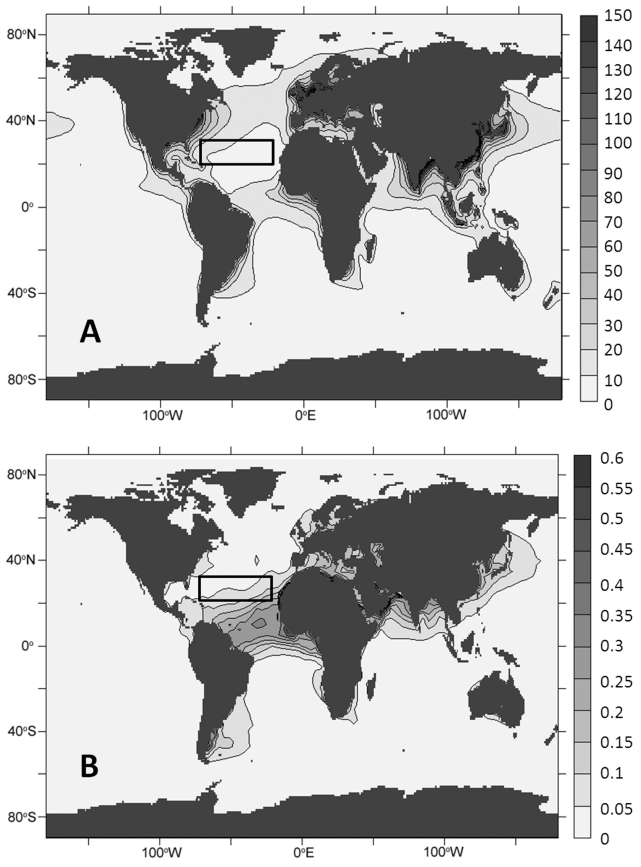

Fig. 4. Modeled atmospheric deposition to the North Atlantic. **(A)** Inorganic N deposition (mmol N m^{-2} yr^{-1}) **(B)** total P deposition (mmol TP m^{-2} yr^{-1}). The NASTG region is outlined.

2.2 Circulation model

Global ocean circulation was simulated by the Modular Ocean Model Version 4p0d (MOM4) from the Geophysical Fluid Dynamics Laboratory (GFDL) in Princeton, New Jersey. The MOM4 model was driven by climatological forcing following the Coordinated Ocean Reference Experiments (CORE) (based on Large and Yeager, 2004). Model configuration corresponds to that used in GFDL's coupled climate model CM2.1 (Griffies et al., 2005; Gnanadesikan, 2006). The model was initialized with annual mean temperature and salinity from the World Ocean Atlas 2001 (Boyer et al., 2002; Stephens et al., 2002) and was run with a $2^\circ\times3^\circ$ horizontal resolution and 28 vertical layers. Atmospheric N and P, interpolated from the monthly deposition maps described above, were added to the uppermost grid box. Year 2000 deposition was applied in amounts corresponding to Fig. 4a and b each year that the model ran. Although deposition was applied over the entire global ocean, we can neglect the impact of atmospheric deposition in other ocean basins because it would take longer than the 70 years of the model run for deposition in other basins to affect the biogeochemistry of the North Atlantic.

Seawater density is an indicator of the physical transport processes that affect the DINxs pool distribution. Modeled and observed upper ocean density distributions compared

favorably (e.g. Fig. 5), suggesting that the model captured the important physical processes in the NASTG.

2.3 Biogeochemical model

Ecological interactions were simulated with a nutrient-phytoplankton-zooplankton-detritus (NPZD) type model similar to the one described in (Oschlies and Garçon, 1999). Modifications were made to increase the sinking speed of detritus linearly with depth (following a modified version of Eq. (6) in Kriest and Oschlies, 2008). After spinning up the physical model for 20 years, the ecosystem and circulation models were coupled online and run for 70 years with atmospheric deposition. The six prognostic biogeochemical variables were nitrate, phosphate, non-diazotrophic phytoplankton, zooplankton, and particulate detritus (one variable for detrital phosphorus and another for detrital nitrogen). Initial oceanic concentrations of nitrate, phosphate and oxygen were obtained from the World Ocean Atlas (WOA) 2001 (Conkright, 2002; Locarnini et al., 2002). Phytoplankton, zooplankton and detritus concentrations were obtained using a mmol N:mg chlorophyll ratio of 1.59 and setting initial detritus and zooplankton concentrations as 1% of the initial phytoplankton concentration. In the Redfield scenario, phytoplankton, zooplankton, and detritus are all simulated as the respective nitrogen equivalents, and phosphorus and oxygen fluxes are diagnosed from the nitrogen fluxes by applying the respective Redfield ratios. Export flux was determined from the product of detritus concentrations with the sinking velocity at approximately the base of the euphotic layer (100 m). The supplementary material provides a concise description of our ecosystem model and chosen parameters (see http://www.biogeosciences.net/7/777/2010/bg-7-777-2010-supplement.pdf).

For comparison, a finer resolution model ($1^\circ \times 1^\circ$ horizontal resolution and 50 vertical layers) was run for 42 years for the Redfield scenarios and compared to the coarser resolution runs. Within the NASTG region (20–32 N, 25–75 W), the one degree model NO_3^- and PO_4^{3-} nutriclines were similar in shape to the coarse model except that differences in surface physics depressed the nutrient gradients by about 50 m in the top 200 m (Fig. 6). This depression of the nutricline did not affect the magnitude of the nutrient deposition signal between 200–800 m for NO_3^-. At the end of the fine resolution model run, nutrient deposition caused an accumulation of 0.80 mmol NO_3^- m^{-3}, whereas in the fine resolution model there was an accumulation of 0.78 mmol NO_3^- m^{-3} at year 42. Because the nutrient deposition accumulation signal includes both the physical and biological dynamics relevant to this study, the 3% difference between the fine and coarse models was small enough that we determined that running the model at a finer resolution was acceptable. For computational reasons, the coarse resolution model was used for the sensitivity studies described in the remainder of the study.

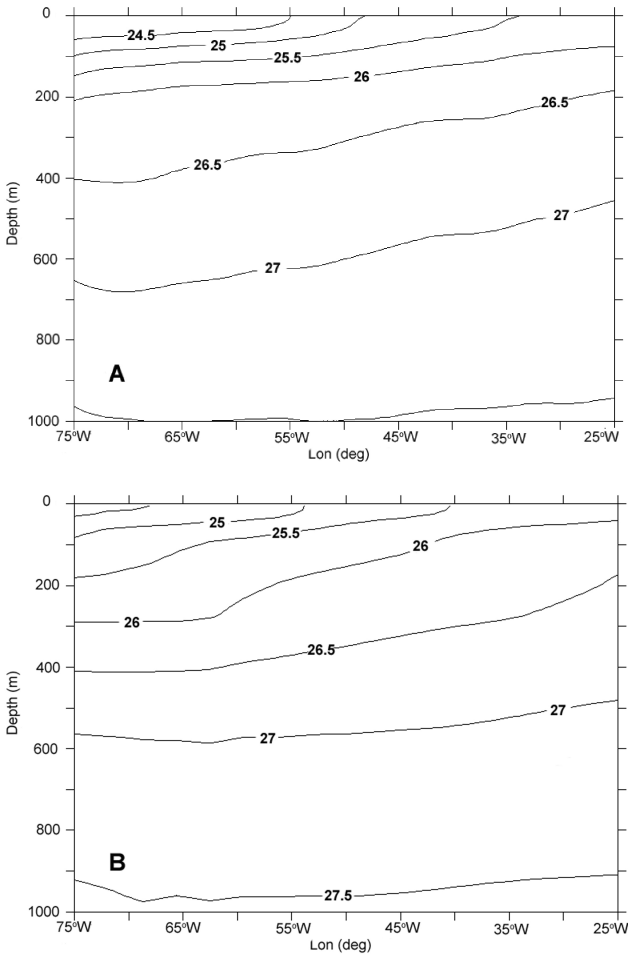

Fig. 5. Zonal cross-sections of density at 24.5° N **(A)** for World Ocean Atlas (WOA) and **(B)** for modeled data after 70 years of simulations.

As described earlier, two non-Redfieldian processes were simulated separately as mechanisms for excess N formation: preferential P remineralization of sinking particles and excess N uptake and export. In the preferential P remineralization scenario, detrital P was given a faster remineralization rate than detrital N in the euphotic layer (0.1 day^{-1} vs. 0.05 day^{-1}, respectively, Oschlies and Garçon, 1999). To ensure that DINxs profiles were realistic at depth, faster preferential remineralization of P occurred only in the euphotic zone (where the majority of labile organic P is thought to be regenerated, Canellas, 2000). This condition required adding to the standard model a separate detrital phosphorus compartment.

In the excess N uptake scenario, our aim was to find the maximum amount of atmospheric DINxs that could be transported to the main thermocline from high N:P particles. For complete export to occur, we assumed two instantaneous processes: first, uptake of all atmospheric excess N by biogenic particles at the ocean surface (which would thereby increase

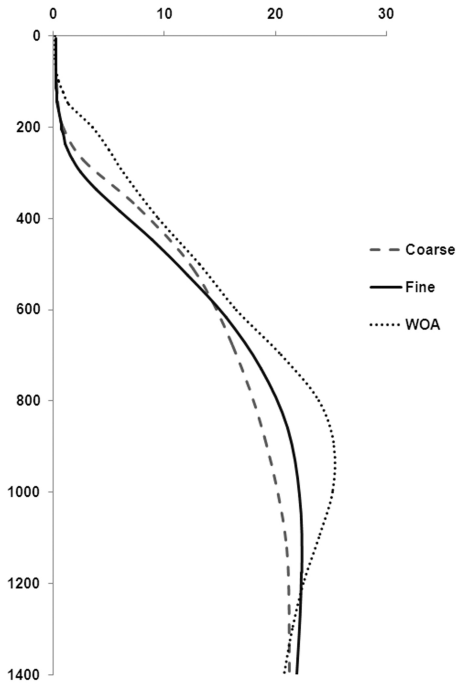

Fig. 6. Average nitrate concentrations (mmol m^{-3}) in the NASTG for WOA data and for the coarse and fine resolution Redfield models with deposition at year 42.

their ratios to greater than Redfield); and second, the export and remineralization of these particles. Given these assumptions, we simulated the effect of atmospherically-derived high N:P particles on ocean biogeochemistry. Beginning at 100 m depth, where we assume that particles begin to remineralize upon export from the euphotic zone, we instantaneously distributed the deposited nutrients into the remineralization zone. The amount of mineralization at a given depth follows the average particulate organic matter remineralization profile in the model. The biogeochemical assumptions specific to the excess N scenario allow no time delay between atmospheric deposition into the surface waters and export of the deposited matter to the ocean interior. This assumption neglects any lateral transport that the particles may experience in the real ocean before remineralization. However, the focus of our study was on long-term changes and so the lack of time delay should not change the maximum effect deposition has on the DINxs pool if deposition increased N:P ratios in surface biogenic particles.

2.4 Isolation of the effects of nutrient deposition on ocean biogeochemistry

Denitrification, DOM formation and remineralization, and N_2 fixation were not explicitly included in the model due to our incomplete understanding of these non-Redfieldian processes in the gyre. Excluding denitrification should not greatly affect the results presented here because denitrification is not thought to be significant in the open North Atlantic water column (Hansell et al., 2007) and although data are scarce, continental shelf denitrification has not yet been demonstrated to have an effect on DINxs concentrations in the subtropical North Atlantic.

However, N_2 fixation is known to be important to the North Atlantic biogeochemistry. We could not realistically model N_2 fixation in the North Atlantic by simply assuming that diazotrophs have an advantage in surface waters with low excess N, i.e. a surplus of P over N (Deutsch et al., 2007; Schmittner et al., 2008). The exclusion of N_2 fixation meant that we could not reproduce the observed DINxs pool nor maintain a realistic steady state of DINxs in the NASTG. Models such as that of Coles and Hood (2007) have dealt with the difficulty in maintaining realistic diazotroph levels by assuming that N_2 fixation equals the rate of development of the excess N signal. Since the goal here was to isolate the atmospheric contribution to the DINxs signal, this mass balance method was not an option. We therefore did not include N_2 fixation in any of the model simulations.

Instead, we compared model runs that did and did not include deposition. The difference between the replicates with and without deposition was taken as the isolated effect of deposition for that scenario. All other complexities within the system, such as those stemming from the lack of N_2 fixation and denitrification, were the same for each replicate. Therefore, the only differences between the two replicates were the exclusive effects of atmospheric deposition. The major assumption of this method is that the various sources of DINxs are sufficiently independent to be superimposed linearly (see Fig. 7) (e.g. N_2 fixation does not affect ocean response to atmospheric deposition and vice versa).

The potential of this assumption to affect our study results depends on whether deposition is sufficiently independent from the process of N_2 fixation to be superimposed linearly as we do in our model. If our assumption that the biogeochemical effects of N_2 fixation do not have any interactions with the biogeochemical impacts of atmospheric deposition is correct, then omitting the N_2 fixation source of excess N has no bearing on the formation of high DINxs from atmospheric deposition and thus, can be ignored. However, if atmospheric deposition does affect N_2 fixation in a major way, or if N_2 fixation affects the oceans response to atmospheric deposition, then our model would have an unquantified source of error. One way that atmospheric deposition could affect N_2 fixation could be by providing Fe (e.g. Moore et al., 2009). Alternatively, N from deposition could enable other organisms to outcompete diazotrophs. We currently do not understand these opposing interactions very well, and cannot include them in our model at this time. Therefore, our results must be interpreted with some caution. However, the main goal of this study is to understand the maximum potential role of atmospheric deposition in DINxs development. While uncertain feedbacks between N_2 fixation and atmospheric deposition probably affect the role of ADINxs

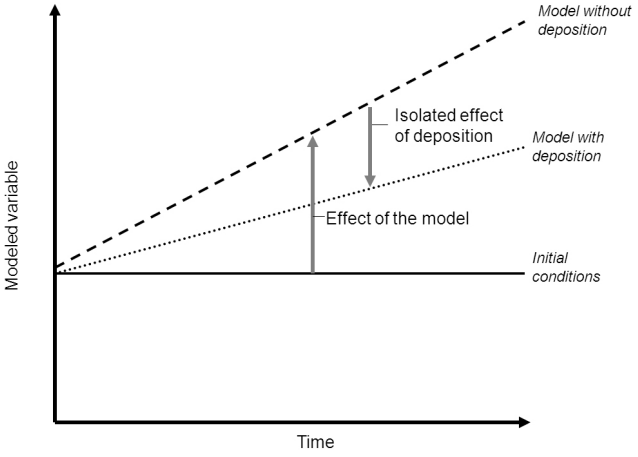

Fig. 7. An illustration of how the effect of deposition on a modeled variable (e.g. phosphate, nitrate, detritus, etc.) is determined. Over time, in this hypothetical case, the modeled variable strays from the initial conditions (for example, because of an inability to accurately model N_2 fixation and DOM). Assuming that atmospheric deposition affects the modeled variable independently of the absence of N_2 fixation and DOM, then the effects of deposition on the system can be isolated despite these deviations from initial conditions. After subtracting the model run without deposition from the run with deposition, we observe, in this hypothetical case, that deposition causes a net decrease in the modeled variable over time.

in the main thermocline, the likely mechanisms of ADINxs transport remain the same.

A DOM compartment was also not explicitly modeled in this study because there are many uncertainties regarding DOM remineralization rates, distributions, and the relative importance of each of these processes on non-Redfield DOM formation. However, the indirect effects of DOM were included in ADINxs estimates. As our focus is purely on the biogeochemical effects of atmospheric deposition, DOM is primarily relevant to this study as a reservoir for high ADINxs. A non-Redfield DOM reservoir can be formed through three processes: atmospheric deposition, N_2 fixation, and preferential P remineralization (Landolfi et al., 2008). It is realistic to assume that within the fraction of DOM which is labile (i.e. which is available to surface biology on timescales shorter than a year), the DOP fraction would cycle faster than the DON fraction (Vidal et al., 1999; Abell et al., 2000; Aminot et al., 2004). Therefore, the effects of non-Redfield DOM on ADINxs development would be included in the preferential P remineralization scenario. Alternatively, if DOM is refractory (i.e. not taken up by biology at the surface until timescales of greater than a year), then the effect of DOM on DINxs would be mimicked by the Redfield scenario. Upon subduction of surface water, transects of DON in the North Atlantic indicate that the majority of subducted DON remineralizes within 15 years (Hansell et al., 2007). Therefore, within the 70 year timescale of our model study,

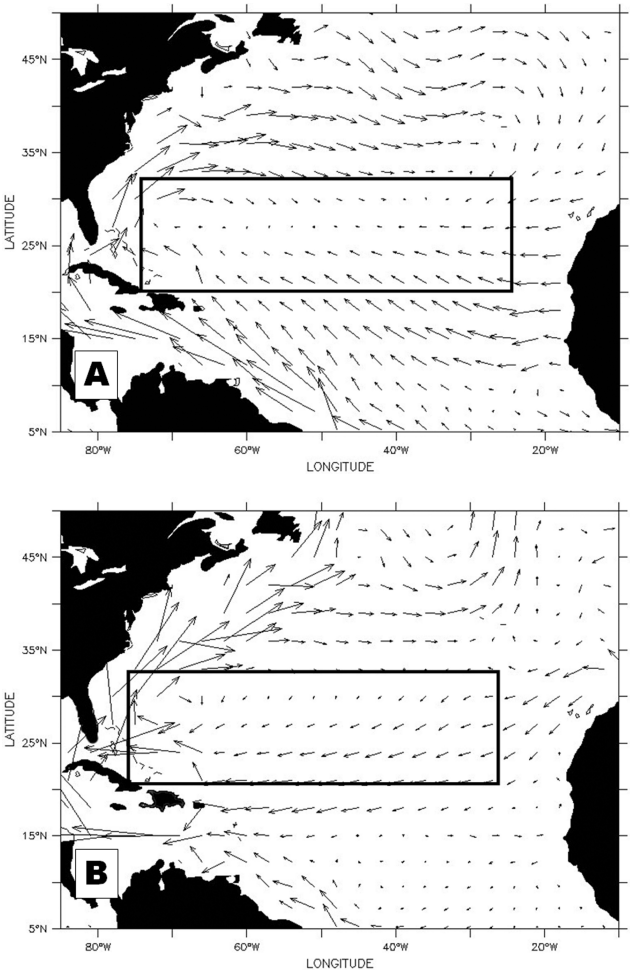

Fig. 8. Modeled year 70 circulation of the NASTG at **(A)** 5 m depth and **(B)** 500 m depth. The NASTG region is outlined.

remineralized DOM should create inorganic nutrient patterns similar to those in the Redfield scenario. Although the preferential P remineralization and Redfield scenarios do not provide any indication of which fraction (organic or inorganic) ultimately contributes the most to the ADINxs signal, they do indicate both the location and the overall contribution of the original atmospheric deposition source to ADINxs.

2.5 Production and loss rates of excess N

Model-simulated surface currents encircled the gyre approximately within the region defined by 20° N to 32° N and 25° W to 75° W (Fig. 8a). In this paper, the NASTG is taken to be the area within this region. The vertical zone of interest was defined as the depth range between 200 and 800 m. Although DINxs essentially moves along isopycnal (i.e., equal density) surfaces once it is formed, for several reasons we used depth surfaces instead of density surfaces as a vertical criterion. Firstly, the remineralization of sinking particles is one of the main vertical transport mechanisms of DINxs in

our simulations. Sinking particles do not follow density lines but rather move through them vertically as they sink, making the degree of remineralization of these particles more related to depth than density. Secondly, the DINxs pool is bounded by different isopycnal surfaces in the western part of the gyre than in the eastern part because isopycnal surfaces deepen from east to west in the gyre while mineralization occurs at more uniform depths (Hansell et al., 2004). Finally, as the isopycnal layers deepen to the west, they mix with South Atlantic water, which masks the growth of DINxs there if density criteria are used (Hansell et al., 2004).

Within the NASTG region, a mass balance technique was used to approximate the production and loss rates of total DINxs. Assuming denitrification to be negligible, the only loss of DINxs is physical transport out of the NASTG. The model's circulation was applied to the observed DINxs field in the gyre in the absence of any DINxs inputs to estimate the loss from physical transport. The change in the observed DINxs pool was computed over a period of five years. Assuming that the North Atlantic is in steady state, we approximated the production rate of DINxs by equating it to the net loss rate of DINxs by transport out of the NASTG.

Lastly, we compared the relative importance in each scenario of ADINxs input to total DINxs pool formation. About 55 years after nutrient deposition began, ADINxs accumulated at a constant rate between 200–800 m. We determined the mean annual growth of ADINxs in the subsequent 15 years, and this rate was taken to be the annual input rate of ADINxs into the gyre's main thermocline.

3 Results and discussion

3.1 Atmospheric nutrient deposition

Annually, there were $9.2\,\mathrm{mmol\,N\,m^{-2}\,yr^{-1}}$ and $0.064\,\mathrm{mmol\,P\,m^{-2}\,yr^{-1}}$ deposited to the NASTG, which, with an average ratio of 143:1, is much greater than the Redfield ratio. Although the original intent of assuming that all deposited phosphorus was bioavailable was to overestimate SRP deposition (Sect. 2.1), modeled P deposition actually slightly under-represented observed wet SRP deposition (dry SRP deposition was not compared due to scarcity of data). The model reproduced 67±43% of observed wet deposition SRP and only 19±35% of observed TP deposition (based on the references in auxiliary material Table S2b in Mahowald et al., 2008, as presented in Fig. 9). As the initial objective was to represent SRP values and not total deposited P, a 67% matchup between modeled P deposition and observed SRP deposition was deemed acceptable. However, an under-representation of P could result in errors in the magnitude of excess N deposition.

Since SRP deposition is usually 2–3 orders of magnitude smaller than soluble inorganic N deposition (e.g. Markaki et al., 2003; Chen et al., 2007), our errors in SRP deposition estimation should have only minor effects on the amount of excess N in deposition. The southeast corner of the basin has the lowest modeled N:P ratio and it is only there that P fraction errors may be non-negligible. However, N:P ratios are still expected to be greater than Redfield (with deposition ratios of at least 37N:1P in the SE corner of the gyre and up to 310N:1P in the NW corner of the NASTG). The effects of atmospheric P on primary production itself is not the focus of this paper, but is assumed to have a relatively minor effect on marine ecosystem productivity on decadal time scales (Michaels et al., 1996).

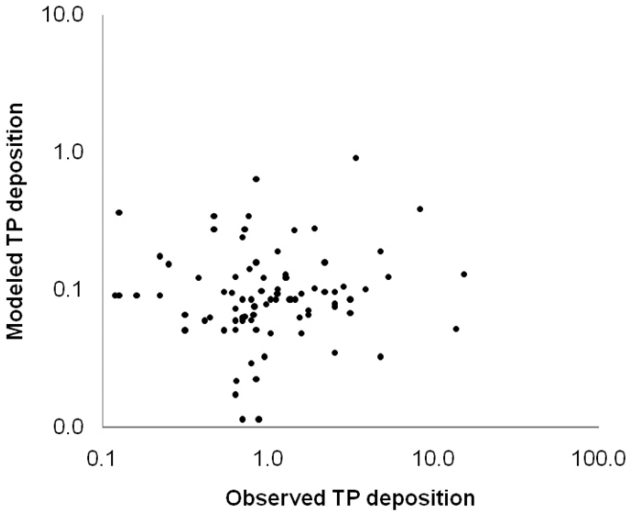

Fig. 9. A scatter plot comparing worldwide total P deposition observations and model estimates ($\mathrm{mg\,m^{-2}\,yr^{-1}}$).

3.2 Excess nitrogen production

3.2.1 Accumulation rates of DINxs in the NASTG

Based on loss rates of observed DINxs transported by the model's circulation out of the NASTG box (Sect. 2.5) and the assumption of steady state, annual DINxs productivity in the NASTG was estimated to be $2.7\times10^{11}\,\mathrm{mol\,N\,yr^{-1}}$. This production rate can be compared with a previous independent estimate for the North Atlantic of $7.8\pm1.7\times10^{11}\,\mathrm{mol\,N\,yr^{-1}}$ (Hansell et al., 2007). The Hansell et al. (2007) estimate was calculated from excess N spatial gradients and ventilation rates within the main thermocline of the North Atlantic. Because their estimate was calculated for the area over which the main thermocline is ventilated, it included sites that produce DINxs outside of the area defined in this study as the NASTG. This difference in areas may explain why our DINxs production rate was smaller than the Hansell et al. (2007) estimate. For the rest of this discussion, we use our modeled production rate.

Table 1. Comparison of observed deposition fluxes of TP and SRP in wet deposition with our modeled TP deposition flux (mg m^{-2} yr^{-1}).

Lat. (N)	Long. (E)	Average annual wet deposition (cm)[a]	n	Observed wet SRP deposition	Modeled wet TP deposition	Reference
36.6	34.3	59	61	8.20	4.83	Özsoy (2003)
36.0	121.0	70	198	23.56	4.75	Zhang et al. (2007)
30.8	123.0	140	75	2.78	4.30	Zhang et al. (2007)
35.3	25.4	55	41	2.21	3.33	Markaki et al. (2003)
32.8	35.1	36	179	9.15	3.45	Herut et al. (1999)
31.8	34.7	18	57	9.15	3.45	Herut et al. (1999)
32.3	295.3	133	14	3.16	1.02	Graham and Duce (1982)
30.6	275.0	146	<149	1.26	0.99	Grimshaw and Dolske (2002)
30.0	277.8	129	<149	1.89	1.39	Grimshaw and Dolske (2002)
26.5	278.0	133	<149	1.89	1.33	Grimshaw and Dolske (2002)
25.3	279.3	133	<149	2.21	1.07	Grimshaw and Dolske (2002)
28.5	279.4	129	<149	1.58	1.10	Grimshaw and Dolske (2002)
13.2	300.5	77	2	6.94	5.26	Talbot et al. (1986)
−3.3	299.7	240	210	2.84	2.66	Williams et al. (1997)
−35	173	104	7	21.87	0.32	Chen et al. (1985)

[a] Deposition flux is inferred from the average annual rainfall obtained from the precipitation climatology of the Global Precipitation Climatology Project (GPCP) (http://www.jisao.washington.edu/data/gpcp).

Our estimate of the DINxs production rate has inherent errors. The initial DINxs concentrations were subject to analytical and interpolation errors within the initial WOA dataset. An error of 0.56 mmol m^{-3} was computed by taking the average of the standard deviations for each gridded point in the WOA dataset and including compounded analytical error in NO_3^- and PO_4^{3-} measurements. The error thus computed is likely to overestimate the error because it includes the variance both within and among sampling stations. Another uncertainty was in our assumption of steady state. The quantity of surface water that enters the main thermocline through springtime mode water subduction is highly variable interannually, affecting DINxs production and dilution in the main thermocline (Bates and Hansell, 2004). Therefore, the degree to which the WOA data represent a system in steady state depends on how well data from the individual cruises that made up the WOA dataset approach the DINxs climatic mean. However, this DINxs production rate can be used to approximate the importance of ADINxs (the atmospheric contribution to DINxs) to the total DINxs pool.

In the model scenarios, it took 55 years to reach a stable ADINxs accumulation rate between 200–800 m in the NASTG region. After this point, the Redfield, preferential P remineralization, and excess N uptake scenarios contributed, respectively, 18±0.5, 13±0.4, and 9±0.5 µmol ADINxs m^{-3} yr^{-1} on average to sustain the DINxs pool with a direct atmospheric deposition of 5.4×10^{10} mol excess N yr^{-1} to the NASTG. Respectively, these contributions equal 27, 19 and 13% of the annual total DINxs production rate.

3.2.2 Spatial distributions of accumulation

We briefly outline NASTG hydrography here because the spatial biogeochemical impacts of nutrient deposition are highly influenced by regional currents and subduction. The NASTG is bounded to the west and northwest by the Gulf Stream. In the northwestern part of the gyre (north of ∼19° N and west of 45° W), spring subduction of subtropical mode water (18° water) ventilates the main thermocline to mean depths of about 287 m with a mean thickness of about 200 m (Peng et al. (2006) and references therein). The NASTG is bounded to the north by the eastward propagating North Atlantic current (between ∼ 30–40° N). Another subduction zone (Madeira mode water) is found northeast of the NASTG between Madeira and the Azores front, subducting south/southwestward along the isopycnal surface σ_θ=26.5 (Seidler et al., 1987). At 35.6° N, dense Mediterranean outflow water enters the North Atlantic and flows south and west between 600–1500 m (Baringer and Price, 1997). Along its southern boundary, the NASTG is ventilated by cross equatorial flow. Within the gyre (centered around 20° N, 35° W), warm salty water subducts inside of the upper thermocline (∼ upper 200 m) to form subtropical underwater (O'Connor et al., 2005).

The location of the ADINxs accumulation rate maximum between 200–800 m was spatially distinct from that of the majority of other DINxs sources. As discussed in Sect. 2.5, by assuming steady state, we defined DINxs production rates as equal, but opposite in sign, to the DINxs loss rates. By this definition, most DINxs was produced in the southern and western parts of the gyre (Fig. 10a). In contrast, most

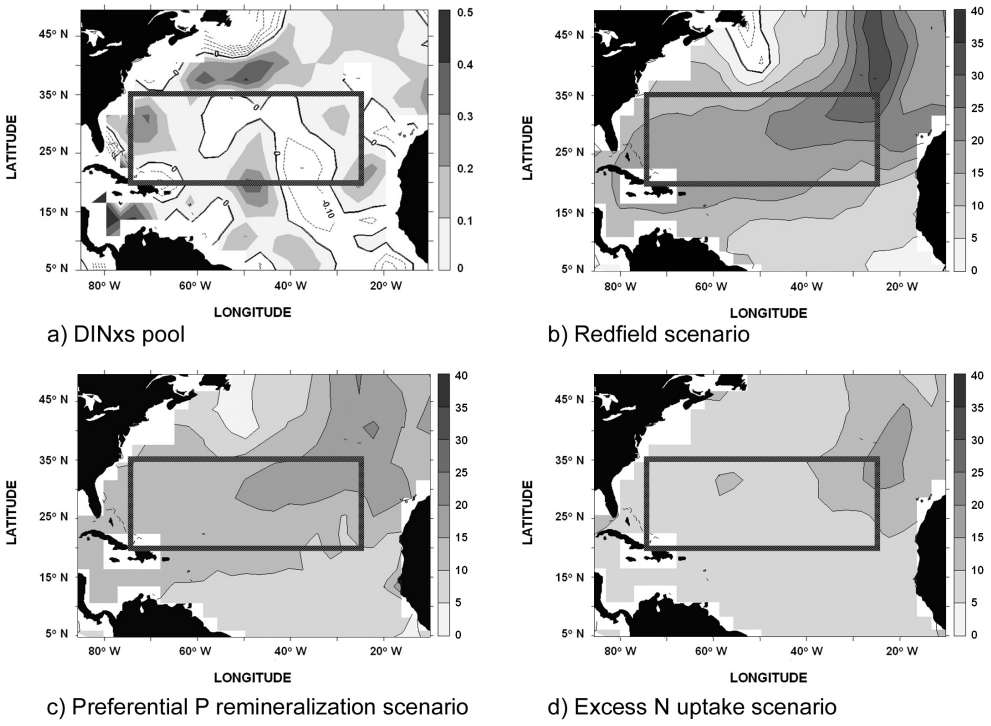

Fig. 10. Average accumulation rates between 200–800 m of **(a)** the total DINxs pool (mmol m^{-3} y^{-1}), and **(b–d)** the atmospheric contributions to the DINxs pool (ADINxs) in the three different scenarios (mg m^{-2} yr^{-1}). The NASTG region is outlined.

atmospheric N deposition originated in North America and was deposited into the northwestern NASTG (Fig. 4a).

As illustrated in Fig. 10b–d, mean ADINxs accumulated at different rates for each scenario but the location of the accumulation rate maximum was the same. The different rates were caused by the unique biological interactions with atmospheric nutrients at the surface in each scenario (described in detail in Sect. 3.3). While biological interactions were important to the overall rate of accumulation, the location of accumulation was mostly determined by the physical transport of water. When surface water nutrient signatures formed from deposition at the surface (Fig. 11), they were then carried to the east by subtropical gyre currents, and were eventually subducted below 200 m in the northeastern part of the gyre. This pattern caused the accumulation of ADINxs to be fastest in the northeast.

When a density layer is used as a vertical criterion instead of a depth layer, similar maxima in ADINxs accumulation rates are observed in the northwest, although for different reasons (Fig. 12). ADINxs accumulates fastest at the surface (Fig. 11), and since isopycnals outcrop at the surface in the northeastern NASTG, the highest rates of ADINxs development were in the east. In contrast to the accumulation rates of ADINxs, the distribution of DINxs production rates within a density layer has a maximum to the west (Fig. 12a) because isopycnals deepening to the west intersect the depth layer that has the greatest production of DINxs.

3.3 Nutrient distributions and transport mechanisms

3.3.1 The Redfield scenario: ADINxs movement by physical transport

So far we have discussed accumulation rates of ADINxs in the three scenarios. Here, we describe the individual effects of each scenario and discuss their differences. We start with the Redfield scenario, in which all biological processes occurred in Redfield ratios so that the only mechanism for ADINxs to accumulate below the mixed layer from the surface is through physical transport of water and the tracers contained in it.

After 70 years in the Redfield scenario without N and P deposition, the absence of N_2 fixation in the model raised surface P to about 3 times higher levels than observed (up to 0.135 mmol m^{-3} P in 70 years from 0.049 mmol m^{-3} in the WOA data). In the Redfield scenario with deposition, the modeled addition of atmospheric nutrients briefly enhanced productivity and export from the surface, but the addition of excess N in the deposited nutrients caused surface P to essentially disappear (Fig. 11b). After P became fully depleted, continued deposition resulted in NO_3^- accumulation in the upper 100 m of the water column. During the 70 year model run, atmospheric nutrient deposition caused surface NO_3^- in the NASTG to increase to levels much higher than currently observed (from WOA conditions of 0.16 to 0.31 mmol m^{-3}).

Although their focus was the global ocean system rather than on the oligotrophic North Atlantic system, the modeling study of Krishnamurthy et al. (2007) also investigated the effects of nutrient deposition on surface biogeochemistry assuming Redfield conditions. Their results from 1990s level deposition likewise denote a global increase in surface N due to deposition (as indicated by a 1–2% increase in global primary productivity from the preindustrial era to the 1990s due to increased N and Fe solubility; Krishnamurthy et al., 2009).

Surface and subsurface circulation (Fig. 8) had a major affect on accumulation of ADINxs in the NASTG. Because most deposited N fell in the west (Fig. 4a), the Gulf Stream swept a sizeable fraction of it out of the NASTG region. However, in the Redfield scenario, ADINxs accumulated in the surface ocean instead of being exported. Therefore, when surface water re-entered the NASTG from the north and east (Fig. 8a), ADINxs from North America (and from Europe) was able to re-enter the gyre in surface and subducted water. Therefore, the Redfield scenario had the highest ADINxs accumulation (and retention of deposited material) in the NASTG between 200–800 m (Fig. 10b). In contrast, vertically exported ADINxs in the non-Redfield scenarios could not easily re-enter the gyre (note the net northward flow of 500 m water away from the northeast sector of the NASTG; Fig. 8b).

ADINxs subduction from surface waters alone cannot realistically explain empirical nutrient patterns in the NASTG, mainly because deposition raises modeled levels of surface N (Fig. 11b) to levels much higher than observed (Fig. 1; Wu et al., 2000; Li and Hansell, 2008). As a result, non-Redfield biological processes are likely to occur during or after assimilation of inorganic N from deposition. Nonetheless, describing the Redfield scenario is useful because it illustrates how nutrient distributions might change if excess N deposition were to become high enough to push the system further towards P limitation. In contrast to the observations, the Redfield scenario does not show the development of a subsurface DINxs maximum in the NASTG region (Fig. 10). Also, although DOM was not specifically considered in this study, the Redfield scenario gives an indication of how subduction and remineralization of DOM will influence DINxs growth because semi-labile DOM should be similarly affected by physical transport as ADINxs in this Redfield scenario.

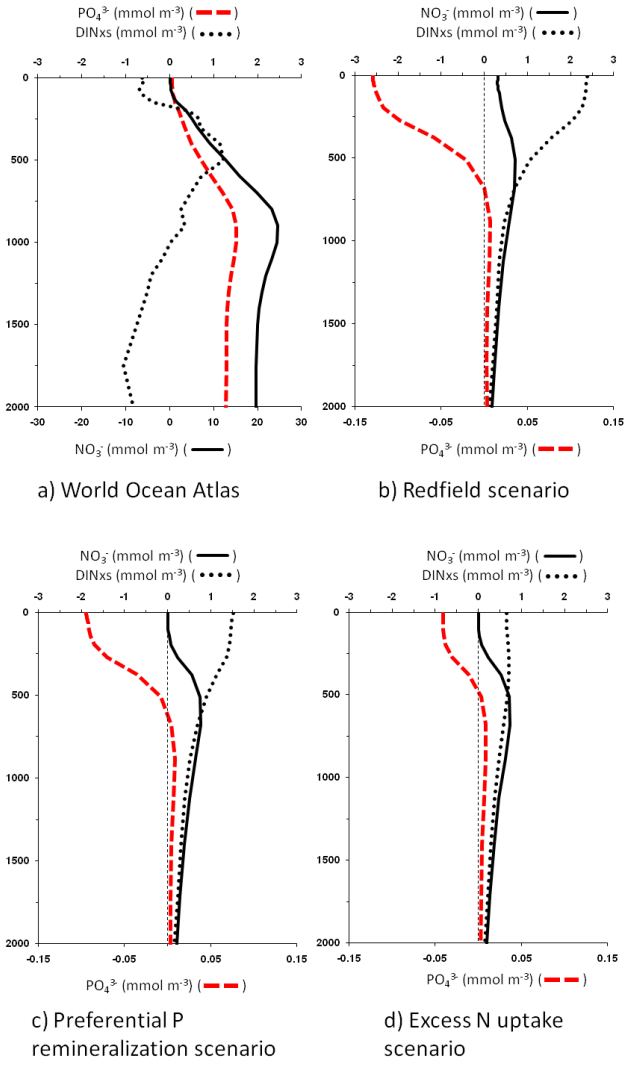

Fig. 11. Average NASTG nitrate, phosphate, and DINxs profiles of **(a)** World Ocean Atlas climatological observations (absolute values), and **(b–d)** the isolated effects of deposition for each scenario at model year 70 (deviation values). Deviations from the dashed line represent differences from the model run with no deposition. The purpose of showing the WOCE data here is to give the reader perspective about the magnitude of nutrient changes due to atmospheric deposition.

3.3.2 The preferential P remineralization scenario: a decoupling of N and P

We next consider how preferential P remineralization affected the distribution of deposited atmospheric nutrients in the ocean. The major difference from the Redfield remineralization scenario was that nutrient deposition did not cause complete P limitation in the surface. Biomass stimulated by deposition grew at Redfield ratios, but P remineralized faster than N when the biomass sank. The result was a spatial separation of remineralized N and P in the water column; of the nutrients taken up by organisms as a result of deposition, the preferential P remineralization run retained an additional 0.5 µmol P m^{-3} yr^{-1} in the NASTG surface compared to the Redfield run, and 13±0.4 µmol ADINxs m^{-3} yr^{-1} grew between 200–800 m (19% of the DINxs volumetric production rate; Sect. 3.2). The excess P in the surface layer allowed additional incoming ADINxs to be available to autotrophs. Thus, nutrient deposition resulted in greater overall nitrogen export from the surface compared to the Redfield scenario and it offered a mechanism by which ADINxs might be transported to depth.

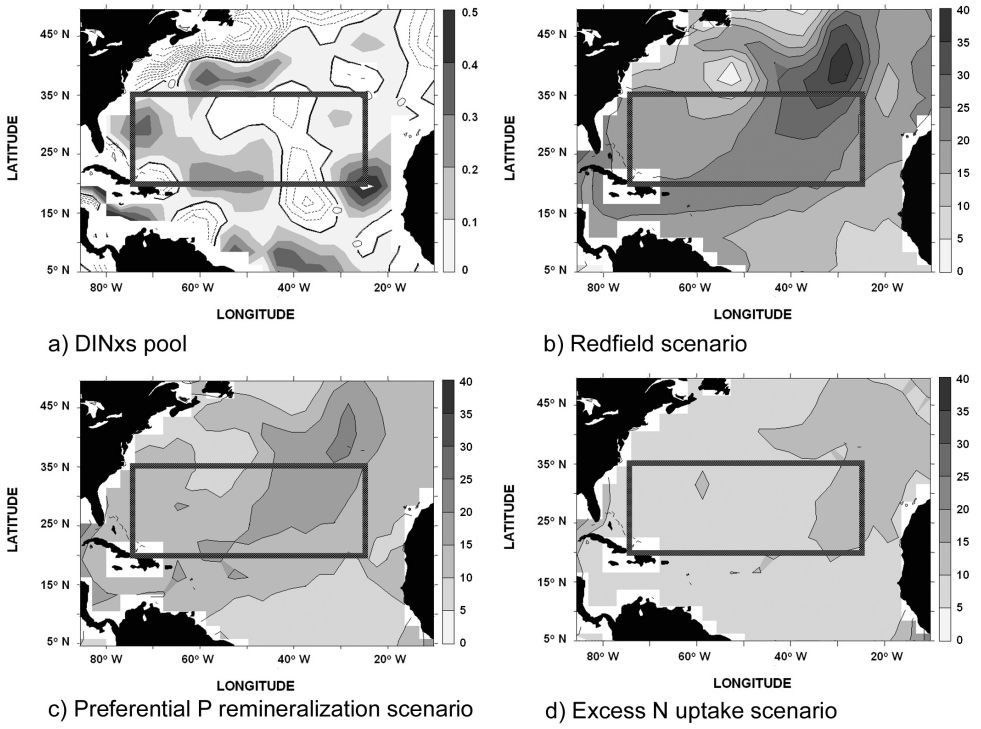

Fig. 12. Average accumulation rates between potential density surfaces σ_θ 26–27 of **(a)** the total DINxs pool (mmol m^{-3} y^{-1}), and **(b–d)** the atmospheric contributions to the DINxs pool (ADINxs) in the three different scenarios (mg m^{-2} yr^{-1}). The NASTG region is outlined.

As discussed in Sect. 2.4, these results are obtained by differencing two preferential P remineralization models: one with deposition and one without. By examining the difference between these two models, we are able to ignore biogeochemical interactions unrelated to deposition. However, in this case, the biogeochemical interactions unrelated to deposition offered interesting insights: we observed that in the models that included preferential P remineralization there were very strong biogeochemical perturbations from WOA conditions. Specifically, surface P increased (illustrated figuratively in Fig. 7) by 0.49 µmol P m^{-3} yr^{-1} over 70 years in the NASTG, even though a decrease in surface P was observed when only the isolated effects of deposition were considered (illustrated as the downward arrow in Fig. 7). This meant that the overall effect of atmospheric excess N was not large enough to balance the excess P generated from production caused by non-deposition sources of nutrients. The signal was large enough that a much higher level of N deposition than modeled here would be necessary to counteract it. With the addition of preferential P remineralization, PO_4^{3-} in the main thermocline remained approximately the same on average as before, increasing a little in the area of the 18° water formation where surface water subducted into the gyre and decreasing in the areas surrounding the gyre. The increase in P at the surface was accompanied by severe N limitation and, as a result of P-rich surface water being subducted, a decrease in DINxs values in the main thermocline from 0.8 to −3.5 mmol m^{-3} after 70 years.

A slower modeled preferential P mineralization rate may reduce differences from WOA conditions. However, the rate of preferential P remineralization used is probably a conservative estimate, based on the rapid turnover rate of phosphorus relative to nitrogen in surface waters (Benitez-Nelson, 2000). We conclude that if preferential P remineralization is to be responsible for the DINxs pool, it must occur in conjunction with one or more sources of excess N at the surface in addition to atmospheric deposition, such as N_2 fixation, in order to balance the excess P generated by preferential P remineralization at the surface.

For previously mentioned reasons, we did not include N_2 fixation in our model. Nonetheless, we can estimate the amount of N_2 fixation necessary in this scenario to sustain observed nutrient patterns in steady state: to balance the excess P at the surface, excess N from N_2 fixation should be equal to 16 times that of excess P. Or, in other words, if preferential P remineralization is the sole mechanism responsible for the high DINxs pool, excess N supplied at the surface from N_2 fixation should have the same magnitude as the amount of DINxs in the main thermocline. In this idealized case, the portion of DINxs that is due to N_2 fixation is 2.3×10^{11} mol N yr^{-1} for the region defined as the NASTG (this value is of course subject to some error because it assumes preferential P remineralization rates are correct and that the DINxs pool is primarily formed due to preferential remineralization).

For realistic nutrient distributions to occur in this scenario, the size of both the DINxs pool, and thereby the amount of N_2 fixation, is directly determined by the rate of preferential P remineralization. Basin-wide, the rate of preferential P remineralization in detritus is not known. We can estimate some upper and lower bounds for remineralization strength to be used in this scenario, by beginning with two assumptions: first, that preferential P remineralization is the only mechanism to contribute to the DINxs pool; second, that the DINxs pool is in steady state in the NASTG. Using an area of $8.13\times10^{12}\,m^2$ (for the NASTG as defined in this paper) and a DINxs production rate of $2.7\times10^{11}\,mol\,N\,yr^{-1}$ (from Sects. 2.5 and 3.2.1), we calculate that sinking particles must produce $0.033\,mol$ DINxs $m^{-2}\,yr^{-1}$ to account for the observed DINxs pool within the NASTG. If all sinking particles were initially at Redfield ratios, the excess N at depth must be balanced by excess P at the surface. Based on our estimate of $0.033\,mol$ DINxs $m^{-2}\,yr^{-1}$, therefore, 0.033/16, or $0.002\,mol$ excess P $m^{-2}\,yr^{-1}$ should be generated in the surface. The strength of preferential P remineralization can then be calculated from the particle flux; the smaller the particle flux, the higher the preferential P remineralization rate must be in order to supply the excess P.

Unfortunately, PON export flux from the NASTG surface to below the euphotic zone is not well constrained. Depending on the method used and the site sampled, N export flux in the NASTG ranges from <0.02 to $0.63\pm0.15\,mol\,N\,m^{-2}\,yr^{-1}$ (Jenkins, 1982, 1988; Jenkins and Goldman, 1985; Oschlies, 2002; Roussenov et al., 2006). If high and low-end estimates of N export and DINxs annual production are used (the latter derived by applying the model's current fields to the observed DINxs distribution, see above), anywhere between 5 and nearly 100% of original P in exported particles would need to remain in the surface. In fact, the low end estimates are too small to account for the DINxs production itself. Given this wide range, we instead primarily focus on export flux and remineralization rates as relevant within our model.

We used a PON export flux of $0.08\,mol\,N\,m^{-2}\,yr^{-1}$, obtained from the first year of the Redfield model in order to approximate the climatological WOA conditions. Given a DINxs production rate of $2.7\times10^{11}\,mol\,N\,yr^{-1}$, we find that $0.003\,mol\,P\,m^{-2}\,yr^{-1}$ is removed from the surface, leaving $0.002\,mol\,P\,m^{-2}\,yr^{-1}$ at the surface as a result of preferential P remineralization. If the DINxs production rate is closer to the Hansell et al. (2007) estimate of $7.8\times10^{11}\,mol\,DINxs\,yr^{-1}$, then the total DINxs signal is larger than the export flux in our model. Having a DINxs signal larger than export flux in our model could indicate that either our export flux value is too small (e.g. because of the neglect of N_2 fixation) or that DINxs is laterally transported into the NASTG.

3.3.3 The excess N uptake scenario: ADINxs movement from high N:P biogenic particles

Finally, we investigated how nutrient distributions would change if biological nutrient uptake did not have to occur in Redfield ratios. In the case of atmospheric deposition, biomass should become N-enriched from the high N:P ratios available in nutrients from deposition. We obtained an upper estimate of ADINxs transport to below the euphotic layer by assuming in our idealized model that all atmospheric nutrients were immediately consumed upon deposition and then exported and remineralized in their original high N:P ratios.

As a result of the model stipulations, the excess N uptake scenario resulted in the most realistic distributions of nutrients. Nitrate and phosphate remained low in the surface and ADINxs developed between 200–800 m (Fig. 11d). Also, surface advection brought in less ADINxs from outside of the gyre since deposited nutrients were immediately removed from the surface waters by export. Therefore, the ADINxs accumulation rate between 200–800 m was smaller than in the other two scenarios (Fig. 10).

One unforeseen result was that we observed a decrease in surface P (Fig. 11d) at a rate of $0.6\,\mu mol\,m^{-3}\,yr^{-1}$; this result was surprising because surface nutrients were not directly altered by deposition. One possible cause for the surface P decrease is the upward mixing of ADINxs from within the subeuphotic zone with surface water, thus supporting surface production that results in the export of P. Consistent with this model observation, surface P in the North Pacific subtropical gyre is higher than in the NASTG (Moutin et al., 2008), perhaps in part because high DINxs water is not upwelled in this system (to the contrary, P-enriched waters underlie the surface Pacific). If export could be modeled in a more realistic way, this upwelled excess N should be immediately exported again once it became available at the surface. However, due to our model stipulations, we could not account for biological uptake in excess of Redfield ratios from upwelled water, and so this observation can probably not be interpreted as similar to what would happen in the real ocean. However, it is interesting that upwelling caused indirect changes in surface nutrients. This result indicates that upwelling may enhance the effect of deposition on the NASTG system because it resupplies ADINxs to the surface.

4 Conclusions

Atmospheric nutrient deposition has long been thought to contribute to the high DINxs development in the North Atlantic (Fanning, 1992; Michaels et al., 1996; Hansell et al., 2007), thereby affecting the geochemical estimates of N_2 fixation in the gyre. Previous works have estimated the various sources of the DINxs pool in the main thermocline of the NASTG, including the contribution from N_2 fixation (Gruber and Sarmiento, 1997; Hansell et al., 2004, 2007; Landolfi

et al., 2008), atmospheric deposition (Hansell et al., 2007; Landolfi et al., 2008), and preferential P remineralization (Landolfi et al., 2008). The work presented here provides the first mechanistic understanding of how deposition might contribute to the development of the observed DINxs pattern, and in this respect, goes beyond the budget-type analysis of pools. We determine that atmospheric nutrient deposition could account for up to 19% of current annual DINxs production rates in the main thermocline and that atmospherically deposited nutrients of natural and anthropogenic origin have probably been affecting DINxs levels in the main thermocline of the NASTG for some time.

Because estimates of nutrient deposition input are still uncertain, there is also considerable uncertainty in how much atmospheric nutrient deposition contributes to high DINxs development in the main thermocline. Due to a paucity of data, we did not include bio-available organic nitrogen and phosphorus deposition in this study. Excluding organic nutrients could potentially lead to a significant underestimation of the effects of nutrient deposition on the ocean. Conversely, the comparison between the modeled phosphorus deposition and the measurements made at various marine-influenced stations tended to underestimate P deposition by ∼40%, which may cause some overestimate of the effects of nitrogen deposition. Accounting for these errors, N:P ratios in deposition will still be consistently higher than Redfield N:P ratios (as expected based on numerous observations). Therefore, even though the magnitude of atmospheric nutrient deposition is somewhat uncertain, we were still able to simulate the direction of biogeochemical effects caused by high N:P deposition to the ocean.

Because modeled purely Redfield conditions produced unrealistic results, we conclude that non-Redfield processes in the surface ocean are essential for the generation of the observed thermocline DINxs signal in the NASTG. Previously, both preferential P remineralization and/or export of particles with high N:P ratios have been suggested as possible mechanisms for exporting excess N from the surface to the main thermocline. Our study, which represents a first attempt to model the interaction of atmospheric nutrient deposition with these non-Redfield processes, reveals that either (or both) mechanisms could be occurring, but that alone, preferential P remineralization would require N_2 fixation or higher levels of deposition to co-occur in order to produce realistic nutrient distributions.

Based on all three modeled scenarios, we also observe that N deposition should be causing P depletion in the surface. This result is supported by the findings of others that indicate that atmospheric deposition is also increasing P limitation in the Mediterranean (Herut et al., 1999), the global ocean (Krishnamurthy et al., 2009), and in lakes (Elser et al., 2009).

Due to the regional rather than global focus of this study, we were able to resolve some of the finer details that affect deposition fate in the NASTG. Deposition location, circulation of NASTG waters, and the rate of local export were very important to the fate of deposition in this region. Rapid ventilation of the gyre enabled atmospherically influenced surface water to be transported to the main thermocline, particularly affecting the northeastern part of the gyre in all scenarios. Because most atmospherically deposited nutrients landed near the Gulf Stream, a rapid export meant that when particles remineralized in deeper waters, they did not re-enter the gyre. In contrast, ADINxs transported in surface waters could re-enter. For this reason and due to the importance of surface water subduction in the NASTG, future studies would benefit by a more comprehensive inclusion of DOM. Finally, from the excess N uptake scenario it appears that convective upwelling may enhance the effects of deposition by resupplying atmospheric nutrients to the surface waters from below.

Some sources of error in this study are the unquantified interactions of atmospheric deposition with DOM and N_2 fixation/denitrification. Although marine DOM is indirectly simulated in the Redfield and preferential P remineralization scenarios, we cannot separate the specific contributions of DOM and inorganic nutrients to ADINxs development, and so any biogeochemical effects due to delayed DOM remineralization in subducting water are unaccounted for. In addition, we did not include interactions between nutrient deposition and N_2 fixation. For example, atmospheric deposition may stimulate N_2 fixation by providing Fe (e.g. Moore et al., 2009). Alternatively, N from deposition could enable other organisms to outcompete diazotrophs. We currently do not understand these opposing interactions very well, and cannot include them in our model at this time; therefore, our results must be interpreted with some caution. Despite the uncertainty in the magnitude of the ADINxs signal, however, this study is the first to provide useful information on the types of effects that atmospheric nutrient deposition has on the North Atlantic subtropical gyre and on the most likely physical and biological mechanisms that affect the fate of deposited nutrients in this region.

Our results support an increasing body of geochemical research that indicates that atmospheric nutrient deposition is important enough to be included in future mass balance assessments of excess N in the NASTG. Based on our results, atmospheric N deposition will probably increase new production and affect surface as well as deep water concentrations of nutrients. Our results reinforce the idea that it is inappropriate to assume Redfield stoichiometry in this area.

Acknowledgements. We thank the AeroCom project (AeroCom Aerosol Comparisons between Observations and Models: http://nansen.ipsl.jussieu.fr/AEROCOM/, access: 2 September 2009) and the Global Precipitation Climatology Project (Merged Satellite, Rain Gauge, and Model Precipitation Estimates: http://www.jisao.washington.edu/data/gpcp, access: 2 September 2009) for use of their data. We also thank the IFM-GEOMAR biogeochemical modeling group, N. Mahowald, D. Olson, J. Prospero, and the two anonymous reviewers for their helpful comments.

L. Zamora and D. A. Hansell were supported by NSF Grant OCE-0623189.

Edited by: J. Middelburg

References

Abell, J., Emerson, S., and Renaud, P.: Distributions of TOP, TON, and TOC in the North Pacific subtropical gyre: Implications for nutrient supply in the surface ocean and remineralization in the upper thermocline, J. Mar. Res., 58, 203–222, 2000.

Aminot, A. and Kérouel, R.: Dissolved organic carbon, nitrogen and phosphorus in the N-E Atlantic and the N-W Mediterranean with particular reference to non-refractory fractions and degradation, Deep Sea Res. I, 51, 1975–1999, 2004.

Antia, A. N.: Solubilization of particles in sediment traps: revising the stoichiometry of mixed layer export, Biogeosciences, 2, 189–204, 2005, http://www.biogeosciences.net/2/189/2005/.

Arrigo, K. R.: Marine microorganisms and global nutrient cycles, Nature, 438, 349–355, 2005.

Baker, A. R., French, M., and Linge, K. L.: Trends in aerosol nutrient solubility along a west-east transect of the Saharan dust plume, Geophys. Res. Lett., 33, L07805, doi:10.1029/2005GL024764, 2006.

Baker, A. R., Jickells, T. D., Witt, M. and Linge, K. L.: Trends in the solubility of iron, aluminum, manganese and phosphorus in aerosol collected over the Atlantic Ocean, Mar. Chem., 98, 43–58, 2006.

Baringer, M. O. N., and Prince, J. F.: Momentum and energy balance of the Mediterranean outflow, J. Phys. Oceanogr., 27, 1678–1692, 1997.

Bates, N. R. and Hansell, D. A.: Temporal variability of excess nitrate in the subtropical mode water of the North Atlantic Ocean, Mar. Chem., 84, 225–241, 2004.

Benitez-Nelson, C. R.: The biogeochemical cycling of phosphorus in marine systems, Earth-Sci. Rev., 51, 109–135, 2000.

Boyer, T. P., Stephens, C., Antonov, J. I., Conkright, M. E., Locarnini, R. A., O'Brian, T. D., and Garcia, H. E.: World Ocean Atlas 2001, Vol. 2: Salinity., 165 pp., 2002.

Bronk, D. A.: Dynamics of DON, in: Biogeochemistry of Dissolved Organic Matter, edited by: Hansell, D. and Carlson, C., Academic Press, San Diego, 153–247, 2002.

Canellas, M., Agusti, S., and Duarte, C. M.: Latitudinal variability in phosphate uptake in the Central Atlantic, Mar. Ecol.-Prog. Ser., 194, 283–294, 2000.

Chen, L., Arimoto, R., and Duce, R. A.: The sources and forms of phosphorus in marine aerosol-particles and rain from northern New Zealand, Atmos. Environ., 19, 779–787, 1985.

Chen, Y., Mills, S., Street, J., Golan, D., Post, A., Jacobson, M., and Paytan, A.: Estimates of atmospheric dry deposition and associated input of nutrients to Gulf of Aqaba seawater, J. Geophys. Res.-Atmos., 112, D04309, doi:10.1029/2006JD007858, 2007.

Coles, V. J. and Hood, R. R.: Modeling the impact of iron and phosphorus limitations on nitrogen fixation in the Atlantic Ocean, Biogeosciences, 4, 455–479, 2007, http://www.biogeosciences.net/4/455/2007/.

Conkright, M. E., Garcia, H. E., O'Brien, T. D., Locarnini, R. A., Boyer, T. P., Stephens, C., and Antonov, J. I.: World Ocean Atlas 2001, Vol. 4: Nutrients, in: NOAA Atlas NESDIS 52, Levitus, S., US Government Printing Office, Washington DC, 392, 2002.

Dentener, F., Drevet, J., Lamarque, J. F., Bey, I., Eickhout, B., Fiore, A. M., Hauglustaine, D., Horowitz, L. W., Krol, M., Kulshrestha, U. C., Lawrence, M., Galy-Lacaux, C., Rast, S., Shindell, D., Stevenson, D., Van Noije, T., Atherton, C., Bell, N., Bergman, D., Butler, T., Cofala, J., Collins, B., Doherty, R., Ellingsen, K., Galloway, J., Gauss, M., Montanaro, V., Muller, J. F., Pitari, G., Rodriguez, J., Sanderson, M., Solmon, F., Strahan, S., Schultz, M., Sudo, K., Szopa, S., and Wild, O.: Nitrogen and sulfur deposition on regional and global scales: A multimodel evaluation, Global Biogeochem. Cy., 20, GB4003, doi:10.1029/2005GB002672, 2006.

Deutsch, C., Sarmiento, J. L., Sigman, D. M., Gruber, N., and Dunne, J. P.: Spatial coupling of nitrogen inputs and losses in the ocean, Nature, 445, 163–167, 2007.

Duarte, C. M., Dachs, J., Llabres, M., Alonso-Laita, P., Gasol, J. M., Tovar-Sanchez, A., Sanudo-Wilhemy, S., and Agusti, S.: Aerosol inputs enhance new production in the subtropical northeast Atlantic, J. Geophys. Res.-Biogeosci., 111, G040006, doi:10.1029/2005JG000140, 2006.

Duce, R. A., LaRoche, J., Altieri, K., Arrigo, K. R., Baker, A. R., Capone, D. G., Cornell, S., Dentener, F., Galloway, J., Ganeshram, R. S., Geider, R. J., Jickells, T., Kuypers, M. M., Langlois, R., Liss, P. S., Liu, S. M., Middelburg, J. J., Moore, C. M., Nickovic, S., Oschlies, A., Pedersen, T., Prospero, J., Schlitzer, R., Seitzinger, S., Sorensen, L. L., Uematsu, M., Ulloa, O., Voss, M., Ward, B., and Zamora, L.: Impacts of atmospheric anthropogenic nitrogen on the open ocean, Science, 320, 893–897, 2008.

Elser, J. J., Andersen, T., Baron, J. S., Bergstrom, A.-K., Jansson, M., Kyle, M., Nydick, K. R., Steger, L., and Hessen, D. O.: Shifts in lake N:P stoichiometry and nutrient limitation driven by atmospheric nitrogen deposition , Science, 326, 835–837, 2009.

Fanning, K. A.: Nutrient provinces in the sea: Concentrations ratios, reaction rate ratios, and ideal covariation, J. Geophys. Res., 97, 5693–5712, 1992.

Galloway, J. N., Howarth, R. W., Michaels, A. F., Nixon, S. W., Prospero, J. M., and Dentener, F. J.: Nitrogen and phosphorus budgets of the North Atlantic Ocean and its watershed, Biogeochem., 35, 3–25, 1996.

Galloway, J. N., Townsend, A. R., Erisman, J. W., Bekunda, M., Cai, Z. C., Freney, J. R., Martinelli, L. A., Seitzinger, S. P., and Sutton, M. A.: Transformation of the nitrogen cycle: Recent trends, questions, and potential solutions, Science, 320, 889–892, 2008.

Gnanadesikan, A., Dixon, K. W., Griffies, S. M., Balaji, V., Barreiro, M., Beesley, J. A., Cooke, W. F., Delworth, T. L., Gerdes, R., Harrison, M. J., Held, I. M., Hurlin, W. J., Lee, H. C., Liang, Z., Nong, G., Pacanowski, R. C., Rosati, A., Russell, J., Samuels, B. L., Song, Q., Spelman, M. J., Stouffer, R. J., Sweeney, C. O., Vecchi, G., Winton, M., Wittenberg, A. T., Zeng, F., Zhang, R., and Dunne, J. P.: GFDL's CM2 global coupled climate models. Part II: The baseline ocean simulation, J. Climate, 19, 675–697, 2006.

Graham, W. F., Piotrowicz, S. R., and Duce, R. A.: The sea as a source of atmospheric phosphorus, Mar. Chem., 7, 325–342, 1979.

Graham, W. F. and Duce, R. A.: The atmospheric transport of phosphorus to the western North-Atlantic, Atmos. Environ., 16, 1089–1097, 1982.

Griffies, S. M., Gnanadesikan, A., Dixon, K. W., Dunne, J. P., Gerdes, R., Harrison, M. J., Rosati, A., Russell, J. L., Samuels, B. L., Spelman, M. J., Winton, M., and Zhang, R.: Formulation of an ocean model for global climate simulations, Ocean Sci., 1, 45–79, 2005, http://www.ocean-sci.net/1/45/2005/.

Grimshaw, H. J. and Dolske, D. A.: Rainfall concentrations and wet atmospheric deposition of phosphorus and other constituents in Florida, USA, Water Air Soil Pollut., 137, 117–140, 2002.

Gruber, N. and Sarmiento, J. L.: Global patterns of marine nitrogen fixation and denitrification, Global Biogeochem. Cy., 11, 235–266, 1997.

Hansell, D. A., Bates, N. R., and Olson, D. B.: Excess nitrate and nitrogen fixation in the North Atlantic Ocean, Mar. Chem., 84, 243–265, 2004.

Hansell, D. A., Olson, D. B., Dentener, F., and Zamora, L. M.: Assessment of excess nitrate development in the subtropical North Atlantic, Mar. Chem., 106, 562–579, 2007.

Herut, B., Krom, M. D., Pan, G., and Mortimer, R.: Atmospheric input of nitrogen and phosphorus to the Southeast Mediterranean: Sources, fluxes, and possible impact, Limnol. Oceanogr., 44, 1683–1692, 1999.

Jenkins, W. J.: Oxygen utilization rates in North Atlantic subtropical gyre and primary production in oligotrophic systems, Nature, 300, 246–248, 1982.

Jenkins, W. J.: Nitrate flux into the euphotic zone near Bermuda, Nature, 31, 521–523, 1988.

Jenkins, W. J. and Goldman, J. C.: Seasonal oxygen cycling and primary production in the Sargasso Sea, J. Mar. Res., 43, 465–491, 1985.

Karl, D. M. and Björkman, K.: Dynamics of DOP, in: Biogeochemistry of Dissolved Organic Matter, edited by: Hansell, D. and Carlson, C., Academic Press, San Diego, 249–366, 2002.

Knapp, A. N., Hastings, M. G., Sigman, D. M., Lipschultz, F., and Galloway, J. N.: The flux and isotopic composition of reduced and total nitrogen in Bermuda rain, Mar. Chem., in press, 2010.

Kriest, I. and Oschlies, A.: On the treatment of particulate organic matter sinking in large-scale models of marine biogeochemical cycles, Biogeosciences, 5, 55–72, 2008, http://www.biogeosciences.net/5/55/2008/.

Krishnamurthy, A., Moore, J. K., Mahowald, N., Luo, C., Doney, S. C., Lindsay, K., and Zender, C. S.: Impacts of increasing anthropogenic soluble iron and nitrogen deposition on ocean biogeochemistry, Global Biogeochem. Cy., 23, GB3016, doi:10.1029/2008GB003440, 2009.

Krishnamurthy, A., Moore, J. K., Zender, C. S., and Luo, C.: Effects of atmospheric inorganic nitrogen deposition on ocean biogeochemistry, J. Geophys. Res.-Biogeosci., 112, G02019, doi:10.1029/2006JG000334, 2007.

Landolfi, A., Oschlies, A., and Sanders, R.: Organic nutrients and excess nitrogen in the North Atlantic subtropical gyre, Biogeosciences, 5, 1199–1213, 2008, http://www.biogeosciences.net/5/1199/2008/.

Large, W. G. and Yeager, S. G.: Diurnal to decadal global forcing for ocean and sea-ice models: The data sets and flux climatologies, Technical Report TN-460+STR, NCAR, 105 pp., 2004.

Li, Q. P. and Hansell, D. A.: Nutrient distributions in baroclinic eddies of the oligotrophic North Atlantic and inferred impacts on biology, Deep-Sea Res. II, 55, 1291–1299, 2008.

Locarnini, R. A., O'Brien, T. D., Garcia, H. E., Antonov, J. I., Boyer, T. P., Conkright, M. E., and Stephens, C.: World Ocean Atlas 2001, Vol. 3: Oxygen, in: NOAA Atlas NESDIS 51, Levitus, S., US Government Printing Office, Washington, DC, 286, 2002.

Lomas, M. W., Swain, A., Shelton, R., and Ammerman, J. W.: Taxonomic variability of phosphorus stress in Sargasso Sea phytoplankton, Limnol. Oceanogr., 49, 2303–2310, 2004.

Mahowald, N. M., Artaxo, P., Baker, A. R., Jickells, T. D., Okin, G. S., Randerson, J. T., and Townsend, A. R.: Impacts of biomass burning emissions and land use change on Amazonian atmospheric phosphorus cycling and deposition, Global Biogeochem. Cy., 19, GB4030, doi:10.1029/2005GB002541, 2005.

Mahowald, N. M., Jickells, T. D., Baker, A. R., Artaxo, P., Benitez-Nelson, C. R., Bergametti, G., Bond, T. C., Chen, Y., Cohen, D. D., Herut, B., Kubilay, N., Losno, R., Luo, C., Maenhaut, W., McGee, K. A., Okin, G. S., Siefert, R. L., and Tsukuda, S.: Global distribution of atmospheric phosphorus sources, concentrations and deposition rates, and anthropogenic impacts, Global Biogeochem. Cy., 22, GB4026, doi:10.1029/2008GB003240, 2008.

Markaki, Z., Oikonomou, K., Kocak, M., Kouvarkis, G., Chaniotaki, A., Kubilay, N., and Mihalopoulos, N.: Atmospheric deposition of inorganic phosphorus in the Levantine Basin, eastern Mediterranean: Spatial and temporal variability and its role in seawater productivity, Limnol. Oceanogr., 48, 1557–1568, 2003.

Michaels, A. F., Olson, D., Sarmiento, J. L., Ammerman, J. W., Fanning, K., Jahnke, R., Knap, A. H., Lipschultz, F., and Prospero, J. M.: Inputs, losses and transformations of nitrogen and phosphorus in the pelagic North Atlantic, in: Nitrogen Cycling in the North Atlantic Ocean and its Watersheds, edited by: Howarth, R. W., Kluwer Academic Publishers, Dordrecht, Boston, 181–226, 1996.

Moore, C. M., Mills, M. M., Achterberg, E. P., Geider, R. J., LaRoche, J., Lucas, M. I., McDonagh, E. L., Pan, X., Poulton, A. J., Rijkenberg, M. J. A., Suggett, D. J., Ussher, S. J., and Woodward, E. M. S.: Large-scale distribution of Atlantic nitrogen fixation controlled by iron availability, Nature Geosci., 2,867–871, 2009.

Moutin, T., Karl, D. M., Duhamel, S., Rimmelin, P., Raimbault, P., Van Mooy, B. A. S., and Claustre, H.: Phosphate availability and the ultimate control of new nitrogen input by nitrogen fixation in the tropical Pacific Ocean, Biogeosciences, 5, 95–109, 2008, http://www.biogeosciences.net/5/95/2008/.

O'Connor, B. M., Fine, R. A., and Olson, D. B.: A global comparison of subtropical underwater formation rates, Deep Sea Res. I, 52, 1569–1590, 2005.

Oschlies, A.: Can eddies make ocean deserts bloom? Global Biogeochem. Cy., 16, 1106, doi:10.1029/2001GB001830, 2002.

Oschlies, A. and Garçon, V.: An eddy-permitting coupled physical-biological model of the North Atlantic – 1. Sensitivity to advection numerics and mixed layer physics, Global Biogeochem. Cy., 13, 135–160, 1999.

Özsoy, T.: Atmospheric wet deposition of soluble macro-nutrients in the Cilician Basin, north-eastern Mediterranean sea, J. Environ. Monit., 5, 971–976, 2003.

Pahlow, M. and Oschlies, A.: Chain model of phytoplankton P, N and light colimitation, Mar. Ecol.-Prog. Ser., 376, 69–83, 2009.

Pahlow, M. and Riebesell, U.: Temporal trends in deep ocean Redfield ratios, Science, 287, 831–833, 2000.

Peierls, B. L. and Paerl, H. W.: Bioavailability of atmospheric organic nitrogen deposition to coastal phytoplankton, Limnol. Oceanogr., 42, 1819–1823, 1997.

Peng, G., Chassignet, E. P., Kwon, Y.–O., and Riser, S. C.: Investigation of variability of the North Atlantic Subtropical Mode Water using profiling float data and numerical model output, Ocean Modell., 13, 65–85, 2006.

Redfield, A. C., Ketchum, B. H., and Richards, F. A.: The influence of organisms on the composition of seawater, in: The Sea, Ideas and Observations on Progress in the Study of the Seas, edited by: Hill, M. N., Interscience, New York, 26–77, 1963.

Roussenov, V., Williams, R. G., Mahaffey, C., and Wolff, G. A.: Does the transport of dissolved organic nutrients affect export production in the Atlantic Ocean?, Global Biogeochem. Cy., 20(14), GB3002, doi:10.1029/2005GB002510, 2006.

Schmittner, A., Oschlies, A., Matthews, H. D., and Galbraith, E. D.: Future changes in climate, ocean circulation, ecosystems, and biogeochemical cycling simulated for a business-as-usual CO_2 emission scenario until year 4000 AD, Global Biogeochem. Cy., 22, GB1013, doi:10.1029/2007GB002953, 2008.

Seidler, G., Kuhl, A., and Zenk, W.: The Madeira mode water, J. Phys. Oceanogr., 17, 1561–1570, 1987.

Seitzinger, S. P. and Sanders, R. W.: Atmospheric inputs of dissolved organic nitrogen stimulate estuarine bacteria and phytoplankton, Limnol. Oceanogr., 44, 721–730, 1999.

Stephens, C., Antonov, J. I., Boyer, T. P., Conkright, M. E., Locarnini, R. A., O'Brian, T. D., and Garcia, H. E.: World Ocean Atlas 2001, Vol. 1: Temperature, 2002.

Talbot, R. W., Harriss, R. C., Browell, E. V., Gregory, G. L., Sebacher, D. I., and Beck, S. M.: Distribution and geochemistry of aerosols in the tropical North-Atlantic troposphere – relationship to Saharan dust, J. Geophys. Res.-Atmos., 91, 5173–5182, 1986.

Taylor, S. R. and McLennan, S. M.: The geochemical evolution of the continental crust, Rev. Geophys., 33, 241–265,1995.

Van Mooy, B. A. S., Fredricks, H. F., Pedler, B. E., Dyhrman, S. T., Karl, D. M., Koblizek, M., Lomas, M. W., Mincer, T. J., Moore, L. R., Moutin, T., Rappe, M. S., and Webb, E. A.: Phytoplankton in the ocean use non-phosphorus lipids in response to phosphorus scarcity, Nature, 458, 69–72, doi:10.1038/nature07659, 2009.

Vidal, M., Duarte, C. M., and Agusti, S.: Dissolved organic nitrogen and phosphorus pools and fluxes in the central Atlantic Ocean, Limnol. Oceanogr., 44, 106–115, 1999.

Williams, M. R., Fisher, T. R., and Melack, J. M.: Chemical composition and deposition of rain in the central Amazon, Brazil, Atmos. Environ., 31, 207–217, 1997.

Wu, J., Sunda, W., Boyle, E. A., and Karl, D. M.: Phosphate depletion in the western North Atlantic Ocean, Science, 289, 759–762, 2000.

Zamora, L., Hansell, D., and Prospero, J.: The organic nitrogen fraction of deposition over the North Atlantic, Geochim. Cosmochim. Acta, 73 (13, Supplement 1), A1498, 2009.

Zhang, G. S., Zhang, J., and Liu, S. M.: Characterization of nutrients in the atmospheric wet and dry deposition observed at the two monitoring sites over Yellow Sea and East China Sea, J. Atmos. Chem., 57, 41–57, 2007.